Available online at www.sciencedirect.com
SCIENCE DIRECT®
Composites Science and Technology 63 (2003) 1561–1569
COMPOSITES SCIENCE AND TECHNOLOGY
www.elsevier.com/locate/compscitech

Load transfer mechanism in carbon nanotube ropes

Dong Qian[a], Wing Kam Liu[b], Rodney S. Ruoff[b,*]

[a]Department of Mechanical, Industrial and Nuclear Engineering, University of Cincinnati, Cincinnati, OH 45221-0072, USA
[b]Department of Mechanical Engineering, Northwestern University, 2145 Sheridan Road, Evanston, IL 60208, USA

Received 6 December 2002; received in revised form 15 January 2003; accepted 20 January 2003

Abstract

We used molecular mechanics and molecular dynamics to study the nature of load transfer in a single walled carbon nanotube (SWCNT) bundle consisting of seven (10,10) SWCNTs: one core tube surrounded by six tubes on the perimeter. The surface tension and the inter-tube corrugation are identified as the two factors that contribute to load transfer. The surface tension effectively acts over a "line" (roughly over the circumference of each tube). The inter-tube corrugation scales linearly with respect to the contact surface area, and increases non-linearly as the inter-tube distance decreases. Relaxation in the nanotube cross-section leads to better inter-tube load transfer as a slight "faceting" develops; the tubes appear to be partially polygonized, rather than perfect cylinders. Compared with parallel bundles, twisting can significantly enhance the load transfer between neighboring tubes; this has been computed as a function of twist angle for this nanotube bundle system.

Keywords: A. Carbon fibers; A. Nanostructures; B. Mechanical properties; B. Modeling; C. Computational simulation

1. Introduction

Carbon nanotubes are a new nanoscale material discovered by Iijima [1]. A significant body of theoretical and experimental work has been devoted to this special material. These studies show impressive physical properties such as high stiffness, high strength, low density, and excellent thermal conductivity [2,3], suggesting a role in light-weight high strength material applications. A comprehensive review of mechanical properties and applications can be found in reference [4]. Two major structural forms of carbon nanotubes are known to exist: single walled carbon nanotube (SWCNT) bundles and multi-walled carbon nanotubes (MWCNT). As shown in the rest of this paper, despite the high stiffness and strength of individual carbon nanotubes, the stiffness and strength of fibers composed of nanotubes are often governed by the inter-tube van der Waals interaction.

The possibility of using SWCNT and MWCNT as reinforcing material for composites has been studied. Significant enhancement in stiffness and strength was reported in a number of experiments [5,6] as compared with bare composites. From the modeling point of view, the improvement in the mechanical properties relies mainly on an effective load transfer mechanism between the composite matrix and the nanotubes, and the load transfer within the nanotube system itself. For a bundle of SWCNT such as the seven-tube bundle of (10,10) tubes mentioned earlier, or for the case of a multi-walled carbon nanotube (MWCNT) with nested, concentric shells, the degree of load transfer between the individual tubes is a relevant issue. This second aspect is the central theme of this paper. An ineffective load transfer within the nanotube system is characterized by a stick-to-slip transition between the nanotube surfaces, which has as an analogy the friction phenomena at the continuum scale. We therefore introduce the concept of nanoscale friction. We further show in the rest of the paper that the mechanics that causes such nanoscale friction differs from the mechanics of continuum scale friction. In order to clearly address this issue, a basic understanding of the structure of the two types of carbon nanotubes, multi-walled vs. single walled, is needed.

MWCNTs are essentially nested shells of SWCNTs. Tensile loading studies of multi-walled carbon nano-

* Corresponding author. Fax: +1-847-491-3915.
E-mail addresses: dong.qian@uc.edu (D. Qian), w-liu@northwestern.edu (W.K. Liu), r-ruoff@northwestern.edu (R.S. Ruoff).

0266-3538/03/$ - see front matter © 2003 Elsevier Ltd. All rights reserved.
doi:10.1016/S0266-3538(03)00064-2

tubes (MWCNTs) attached to opposing AFM cantilever tips and observed with scanning electron microscopy indicated that the outer shell of the MWCNT typically breaks, so that little load transfer occurs to the inner, nested shells [7]. This suggests that the range of potential mechanical applications of MWCNTs may be limited, particularly in situations where the load is primarily being borne only by the outermost shell; with little to no participation from inner shells, the engineering stiffness and strength are low.

The weak inter-shell interaction in several MWCNTs has been measured by Yu et al. [7] and estimated by Cumings and Zettl [8]. In the study of "shell-sliding" of two separate MWCNTs by Yu et al. [7], the dependence of the force buildup during "stick" and the force at each "slip" event, on the contact length between the outermost shells and its immediate neighbor, was measured. This dependence allowed for a fit of the shear strength for the interaction between the outermost shell and the neighboring inner shell, which for two MWCNTs was found to be 0.08 and 0.3 MPa, respectively. These values are on the low end of the experimental values of the shear strength for a range of graphite samples [9], thus emphasizing the weak inter-shell interactions in "high quality, highly crystalline" MWCNTs, similar to the type originally discovered by Iijima [1]. Cumings et al. [8] demonstrated inside a transmission electron microscope (TEM) that a "telescope process" can be repeated on the MWCNTs that they tested up to 20 times without causing any apparent damage. (The reader should note that assessment of damage at the nanoscale is quite challenging. Here, the authors simply noted that there was no apparent change as imaged by high resolution TEM.)

These two studies motivate pondering the possibility of a nanoscale bearing system of exceptional quality. The shear strengths corresponding to static friction and dynamic friction were estimated to be 0.66 and 0.43 MPa, respectively [8], whereas the direct measurement on MWCNT by Yu et al. gave a value for a particular pair of neighboring shells, of 0.08 MPa [7]. Note that the definition of the shear strength used here refers to the maximum shear stress prior to sliding, and the concept of shear stress follows that of engineering stress at the continuum scale, i.e. the load is assumed to be applied to the equivalent surface area of the single atom layer. A case of effective load transfer through the full cross section would occur, for example, for a structure with complete tetravalent bonding of each carbon, such as for single crystal individual diamond nanofibers. Diamond nanofibers could be therefore both much stiffer (at low strain) and have much larger fracture strengths, than MWCNTs [33].

The primary product of current methods of SWCNT synthesis contains not individual, separated SWCNTs, but rather bundles of closest-packed SWCNTs [10,11]. Load transfer to the individual SWCNTs in these bundles is very important for mechanical applications. It is estimated that to achieve load transfer so that the full bundle cross-section would be participating in load-bearing up to the intrinsic SWCNT breaking strength, the SWCNT contact length could be on the order of 10–120 microns [12,13]. There is strong evidence, however, that the typical length of individual SWCNTs in such bundles is only about 300 nm [14,15]. This large gap in terms of contact length means that load transfer in a parallel bundle containing such relatively short SWCNTs is very small and thus ineffective. A quantitative estimate of the contact length based on molecular mechanics is given in the next section.

There are evidently some cases when the SWCNT bundle naturally assumes a twisted form, which is similar to the wire ropes at continuum scale [16]. It is well known from continuum mechanics analysis of other types of wire or fiber forms that twisting the wires or "weaving" the fibers can lead to a cable or rope that has much better load transfer mechanism in tension, than a straight bundle would have [17]. Indeed, the disciplines of textile, and twisted wire, mechanics developed as a way of modeling such structures and designing new twisted structural forms. This motivates the study on the effect of twisting on the load transfer for SWCNT bundles. The understanding we develop from the new modeling we present here should also feedback to developing a deeper understanding of textile and twisted wire mechanics.

2. Load transfer in bundles of parallel SWCNTs

The weak inter-tube interactions in SWCNT bundles have been reported in a number of recent experiments. For instance, a low shear modulus ($\sim$1 GPa) for SWCNT bundles has been measured by Salvetat et al. [18]. In the experiment reported by Ajayan et al. [6], slip rather than breakage of individual SWCNTs was observed in the fracture test of polymers (nominally) reinforced by SWCNT bundles. The energy necessary to produce inter-tube sliding is composed of two parts: the energy to create new free surface (if this is occurring during the inter-tube sliding) and the energy to overcome inter-tube friction, due to the interlayer interactions from neighboring tubes. The interlayer binding energy varies due to "corrugation" effects as inter-tube sliding occurs. A simple estimate of both of the energy terms can be obtained by specifying a particular configuration.

We have used a molecular mechanics (MM) approach to compute the interaction of a SWCNT bundle composed of seven (10,10) SWCNTs. In the MM approach, we simply evaluate the energy and forces based on a fixed configuration and no equilibrium equations are solved. The initial configuration of the SWCNT bundle cross-section is shown in Fig. 1. In Fig. 1, r is the radius

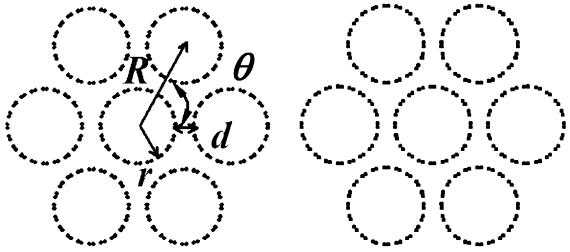

(a) (b)

Fig. 1. Cross-section shape of seven (10,10) tubes in a SWCNT bundle (a) before relaxation and (b) after relaxation.

of the core tube, d is the closest distance between the core and surrounding tube, and R is the center-to-center distance between the core and surrounding tube. The geometric parameters are given as $r = 6.78$ Å, $\theta = \pi/3$, and $d = 3.34$ Å. First, we treat the energetics of pulling out the center tube, in the parallel bundle (no twist). For the purpose of simplification in MM for treating this particular case, we first assume the individual SWCNTs to be rigid. This constraint is then relaxed. The relaxation has a significant effect on the inter-tube contact, as described below. In both rigid and relaxed cases, the binding energy is computed by summing up the inter-tube atom–atom pair energies, using a Lennard-Jones potential (LJ) derived from fitting the interlayer energetics of graphite.

$$\phi_i = \frac{A}{\sigma^6}\left[\frac{1}{2}y_0^6\frac{1}{\left(\frac{r_i}{\sigma}\right)^{12}} - \frac{1}{\left(\frac{r_i}{\sigma}\right)^{6}}\right] \tag{1}$$

In Eq. (1), $\sigma = 1.42$ Å is the C–C bond length, y_0 is a dimensionless constant, and r_i is the distance between the ith atom pair. A cutoff length of 10σ was used in the computation. The parameters for the LJ potential that have been used are from references [19, 20] and are listed in Table 1. Parameter set LJ1 has been used to evaluate the energy of the graphite system, and parameter set LJ2 has been used for calculating the binding energy of C_{60} in the gas and solid phases. For the work described in this paper, the parameter set LJ1 is used.

2.1. Perfect rigid configuration

A "corrugation" effect arises as the core tube is slid incrementally along the axial direction. The binding energy is evaluated during each of the incremental steps. To consider the effect of contact length, we computed the binding energy of atoms located on one hexagonal ring of C atoms that is perpendicular to the axis of the tube (illustrated in Fig. 2). This gives $\bar{\phi} = -0.7$ eV/ring. This energy is then divided by the equivalent length of the ring in the axial direction, which is equal to $\frac{\sqrt{3}}{2}l_{C-C}$ for the (10,10) SWCNT, where l_{C-C} is the carbon bond length. We obtain $\tilde{\phi} = -0.57$ eV/ring for each ring. We define the corrugation effect as the difference between the maximum and minimum values ϕ as the core tube is moved along the axial direction. In this case we obtain a variation of 0.28 meV/Å as a result of a relative displacement of 1.18 Å in the axial direction, which is equivalent to $\tilde{\phi} = 0.24\,\text{meV}/(\mathring{A})^2$. The load transfer can be quantified by the necessary number of rings (thus, the length of contact between neighboring tubes) such that the force (f_1) due to the generation of new surface as sliding occurs plus the force (f_2) to overcome this corrugation effect would equal the force (f) that is needed to break the tube. Note that once the diameter of the tube is assigned, only f_2 scales linearly with the contact length. Therefore,

$$f = f_1 + f_2 = f_1 + l \cdot b_2 \tag{2}$$

with l being the contact length.

For small incremental sliding, Δd, and tubes of finite length, the energy equivalence requires that $\bar{\phi} = f_1\ \Delta d$ and $\tilde{\phi} \cdot l = f\ \Delta d\ l$, which gives $f_1 = 0.57$ eV/Å, $b_2 = 0.24$ meV/(Å)^2. Note that we have assumed that f_1 and f_2 can be considered as constant for such small incremental sliding. Since there are no direct experimental data on the tensile strength of individual SWCNT and theoretical estimations are typically one order higher than the results from indirect testing data [4], we use the values obtained by Yu et al. [21] on the tensile test of the outer shells of MWCNTs, which had 11 GPa for the lower end of the tensile strength. This strength is equivalent to $f = 9.8$ eV/Å for a (10,10) CNT. Solving Eq. (2) yields $l = 3846$ nm. As shown in [14], this value is far greater than the typical contact length (~300 nm) measured for SWCNT samples produced in recent years [10,11]. With an assumed value of 50 GPa for the tensile strength of MWCNT, the estimated length from Eq. (2) is 17.5 μm.

Table 1
LJ parameters

Parameter sources	A (J.m^6)	σ (Å)	y_0
LJ1 [19]	24.3×10^{-79}	1.42	2.7
LJ2 [20]	32×10^{-79}	1.42	2.742

2.2. Relaxed configuration

Although the van der Waals force is weak at low pressure, it does contribute to the radial deformability of individual SWCNTs and thus changes the inter-tube contact. Tersoff and Ruoff [22] studied the deformation pattern of SWCNTs in a closest-packed crystal and concluded that tubes with diameters smaller than 1 nm are less affected by the van der Waals attraction and hardly deform. However for diameters over 2.5 nm the tubes flatten against each other and form a honeycomb-like

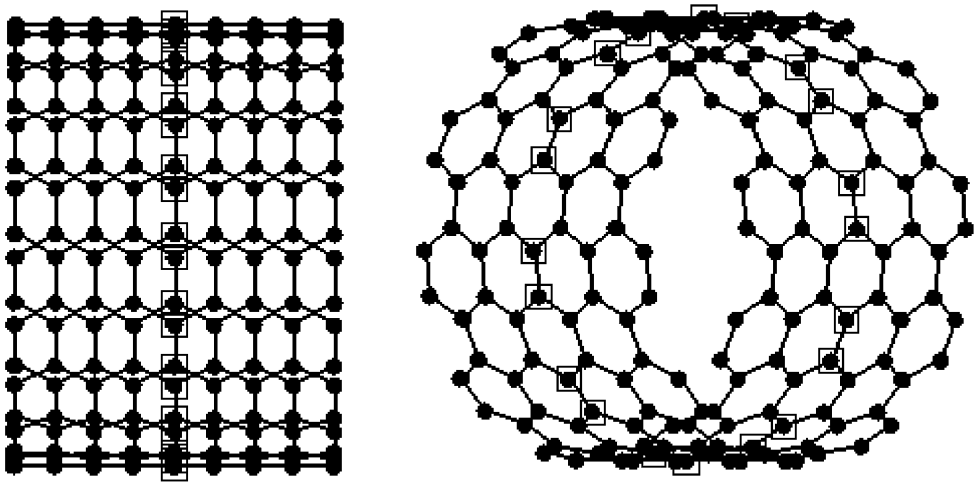

Fig. 2. A section of the (10,10) CNT. (Side view on the left and 3D view on the right). Atoms (marked with a rectangular box) that are located in the same ring perpendicular to the axis are used in the evaluation of energy.

structure. This effect has been confirmed experimentally [32]. This flattening of larger diameter SWCNTs could have a profound effect on the load transfer. Fig. 6 shows at the same scale the cross-sections of a (10,10) SWCNT bundle and a (20,20) SWCNT bundle after being relaxed to equilibrium using molecular dynamics. The MD relaxation scheme presented here and in Section 5.2 is implemented as a NVE ensemble with the use of the conjugate gradient method. Inertia effects are not considered during this process and the final relaxed configuration corresponds to zero temperature. Periodic boundary conditions are assumed in the axial direction for both cases. The "polygonization" process can be clearly seen for the (20,20) SWCNT case, whereas only slight changes in cross-sectional geometry are found for the (10,10) SWCNT case.

These observations from the simulation are in agreement with the conclusions by Tersoff and Ruoff [22]. In the case of (10,10) CNT bundles it is found that the inter-tube distance-of-closest changes from 3.34 to 3.25 Å. Following the same procedure as in Section 2.1 to evaluate the contact length for the (10,10) case, we obtained significantly different results when the relaxation effect is considered. Using the same molecular mechanics approach, we have $f_1 = 0.58$ eV/Å, $b_2 = 0.71$ meV/(Å)^2 for the relaxed case. This yields a critical contact length of $l = 1299$ nm for load bearing at 11 GPa. Although the value is still much longer than 300 nm, it is approximately one third of the estimate given in Section 2.1.

2.3. Effect of shorter inter-tube distance

We further studied the role of pressure by reducing the inter-tube distance d from 3.34 to 3.00 Å while fixing the relaxed cross-section shape for individual (10,10) tubes in the bundle. Because the LJ potential is too "rigid" in the repulsive region, we used an LDA-based Morse potential [23] to treat the 3.00 Å inter-tube spacing. A verification of this model for the high pressure region of graphite is given in [24]. Using this model, we obtained $f_1 = 0.49$ eV/Å, $b_2 = 2.31$ meV/(Å)^2 and contact length $l = 403$ nm, which is close to the 300 nm mean length mentioned earlier. However, to confine the parallel bundle to such a short inter-tube separation for applications would be non-trivial. Based on this Morse potential, Qian et al. [24] obtained an equation of state (EOS) for graphite. A pressure of approximately 6 GPa must be imposed to achieve an interlayer distance of 3.0 Å for the graphite system. For the SWCNT bundle system, this pressure is likely to be smaller due to the curved geometry. For example, it has been shown in the high pressure experiments by Tang et al. [25] that a pressure of only $\sim$1.5 GPa is needed to achieve such an inter-tube gap, although no firm conclusion on the SWCNT chirality was given in Ref. [25]. Note that our estimation is conservative since we ignore the effect of increased pressure on the polygonization process that is demonstrated in Ref. [25]; that is, we have used the "extent of flattening" at zero pressure outlined above, and simply shortened the intertube, as mentioned above.

One may speculate whether sufficient compressive stress (both in the axial and transverse directions) from a surrounding matrix on a perfectly parallel bundle of closest-packed SWCNTs in a polymer/SWCNT bundle composite, could dramatically increase the load transfer between the SWCNTs in the bundle. In this regard, the thermal expansion of SWCNT bundles has been recently measured by variable temperature X-ray diffraction [26]. We take the published value for the thermal expansion of a SWCNT bundle (0.75×10^{-5}), and a typical value for a typical epoxy as 50×10^{-6} and for a polyimide as 90×10^{-6}. A simple analysis on the uniaxial stretch in the polymer matrix reinforced by a single

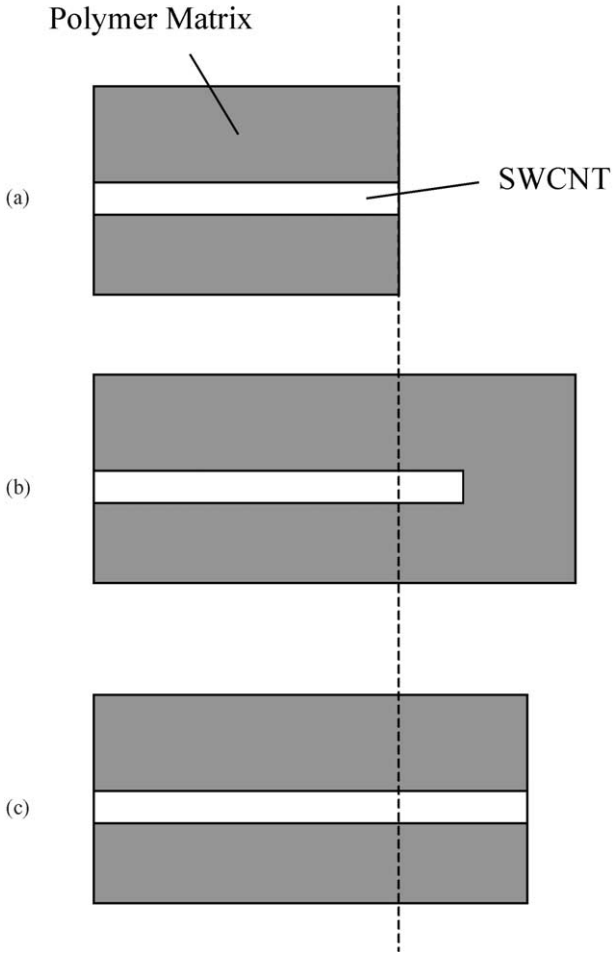

Fig. 3. A simple analysis of uniaxial tension of a polymer reinforced by SWCNT. From top to bottom: (a) initial system; (b) assuming no bonding between the tube and matrix, both will expand under increasing temperature; (c) because of the bonding, the tube will stretch more and the matrix will stretch less compared to (b), which results in compressive stress in the matrix and tensile stress in the tube. An estimate can be obtained by using the SWCNT and polymer thermal expansion coefficients and the kinematic assumption that the SWCNT and polymer have the same expansion as a result of the interfacial bonding.

SWCNT (Fig. 3) results in residual compressive stresses around the bundle in the range of 30–90 MPa, taking into consideration the higher cure and higher stress free temperature of polyimides [27]. The radial stresses exerted on the bundle are compressive, but they are accompanied by equal tensile circumferential (tangential) stresses in the matrix at the interface. Typical tensile strengths of epoxies and polyimides are 70–120 MPa. We note that at 70–120 MPa, there is a very small change in the interlayer separation of neighboring tubes, whether estimated from the *c*-axis compressibility of graphite, or from the recent measurements reported by Tang et al. [25]. It seems that the matrix would crack before any considerable pressure ($\sim$1.5 GPa) builds up on the tube bundle. Thus, it seems unlikely that residual compressive stress in composites will be high enough to cause any significant increase in load transfer between closest-packed SWCNTs. This further emphasizes the importance of forming SWCNT ropes by weaving or twisting, or by their presence in the as-synthesized product, as seen in Ref. [16].

3. Mechanics of wire ropes and relation to SWCNT ropes

Wire ropes are an important structural element and mainly used in applications in which tensile load is dominant as compared to bending or twisting. A wire rope is generally composed of a number of strands and a core, each of which then contains a number of single wires. The rope can be identified by the number and geometric arrangement of the strands surrounding the core. A detailed description can be found in the *Wire Rope Users Manual* [28]. In order to make a distinction, we refer to "rope" for the case of wires that are wrapped helically around a core axis and "bundle" for the case where the wires are parallel to each other. Wire ropes have radial forces (in the direction of vectors $\mathbf{N}$ and $\mathbf{N}'$ as shown in Fig. 4) that press the surrounding wires to the core, and a tangential force (vector τ) that tends to open the strand.

The major advantages of having wires in the form of a rope are:

1. It provides better load transfer and structural reliability. For example, when one wire component breaks, the broken sections of that particular wire can still be bearing load transferred from the other wires, through the strong friction force that is a consequence of the radial compression.
2. Wire rope has a smaller bending stiffness, therefore it is desirable for applications in which the rope has to be frequently bent. The fatigue life is significantly longer.
3. Compared with wires that are in parallel, the structure is stabilized by the radial force component.

Some of these mechanics still hold for the case of SWCNT ropes. For instance, SWCNT ropes are more stable than loosely packed bundles of SWCNTs. However, the treatment of the mechanics differs. Contact forces at the continuum scale for macroscopic wires are now replaced by the interlayer interactions between tubes, often referred to as the non-bonded interaction. In wire rope, the friction force between the contact surfaces is a result of the surface roughness and normal pressure. In SWCNT ropes there is the corrugation effect due to the π orbitals in neighboring SWCNTs. On the other hand, SWCNT ropes also have some unique mechanics that differ from macroscale wire ropes treated on the continuum scale:

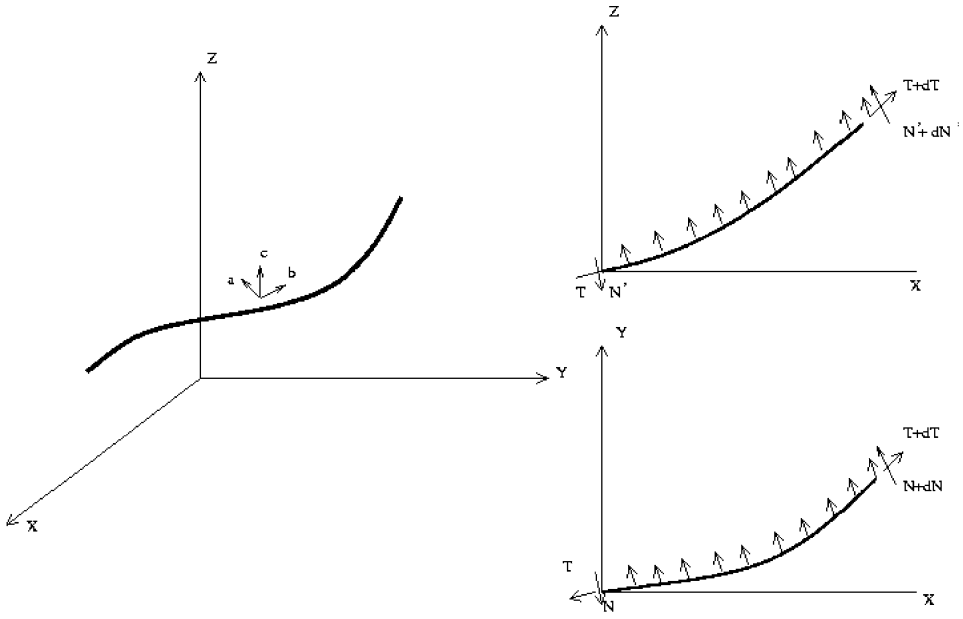

Fig. 4. A 3D section of a wire, and force components in the x–z and x–y planes.

1. In the SWCNT rope, the "strands" are individual SWCNTs that are easier to deform in the radial direction than are solid wires. The radial "squashing" deformability of CNTs is addressed in Ref. [29]. The deformation from circular to collapsed form is strongly affected by the twisting angle, as shown later, and is very different from the case of wire rope (where only small deformation from circular to slightly non-circular cross-section occurs).
2. For these significantly collapsed SWCNTs in highly twisted SWCNT bundles, the effective contact area is significantly changed and this will change the nature of the contact and load transfer.

4. Experimental observation of nanoropes

SWCNTs were dispersed in dimethylformamide (DMF) by sonication in a sonic bath. A micropipette was created in our lab by using a glass-pulling tool. The micropipette was held in a simple clamp that was attached to an *xyz* micropositioning stage. A small amount of the SWCNT DMF dispersion was pulled into the micropipette by capillary action. The tip of the micropipette was then positioned over a home-built testing stage that can be inserted and operated inside a transmission electron microscope. A long focal distance lens (50×, Mitutoyo) was used to observe the positioning of the micropipette tip so that a small amount of the solution could be drawn out of the tip by briefly touching onto the testing stage. The testing stage has a gap of several microns between the force sensing cantilever and a second, opposing ledge. The two opposing ledges are coplanar to a very high degree, because the testing stage is created from a single piece of ~60 μm thick single crystal Si wafer by a multistep fabrication process.

As can be seen from the image in Fig. 5, a small diameter bundle spans the gap. This bundle is comprised of individual SWCNTs. The bundle diameter varies strongly from top to bottom, suggesting that the number of SWCNTs varies in each cross section along the section length spanning the gap. As a consequence of applied tensile load, the SWCNT bundle has "untwined" suggesting that it was actually present as a twisted bundle, perhaps as a consequence of the process of deposition onto the stage.

5. Simulation results

5.1. Effect of inter-tube contact on the cross-section shape

We have used MD based on the empirical Tersoff–Brenner potential [30] to analyze a single strand composed of six (10,10) SWCNTs surrounding a core (10,10) tube, under twist load. The length of each tube is 612 Å and the total number of atoms is 69,860. Before any twist is applied, the tube is first relaxed under periodical boundary condition [see Fig. 1 for the cross-section taken from the middle of the tube (a) before (b) after relaxation]. Both ends of the core tube are then fixed and a twist on the six neighboring SWCNTs around the center of the core is applied at an angular

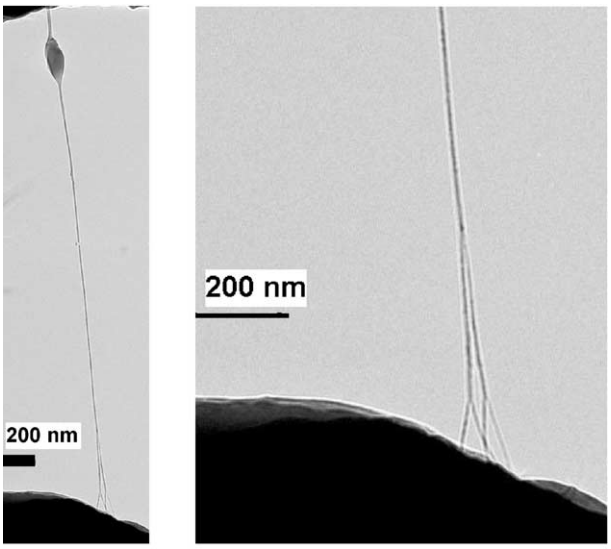

Fig. 5. (a) A SWCNT bundle under tensile loading. (b) Zoom-in image of the untwined SWCNT rope section attached to the platform at the bottom, obtained in a Jeol FX-2000 transmission electron microscope.

velocity of 20 π/ns. The cross-sections of the twisted tubes are fixed at the boundary during the process. The twist is applied such that the atoms on the boundary rotate around the center of the core tube. The geometric parameters are the same as described in Section 2. The Verlet algorithm is adopted for the explicit time integration. The MD is implemented through NVE ensemble with a time step of 0.1 ps. During the process of twisting, an inter-tube gap corresponding to the high-pressure region is present. Similar to the molecular mechanics treatment, we used the same modeling approach for the non-bonded interaction, i.e., using either the LJ potential or the Morse potential based on the inter-tube distance as described above.

Shown in Fig. 7 are three snapshots of the deformation of the bundle after twisting is introduced. The corresponding change in the cross-section is shown in Fig. 8 at the mid-point of the bundle. The deformation is plotted in the same scale as the original geometry. It is observed that the individual CNT's start to collapse in

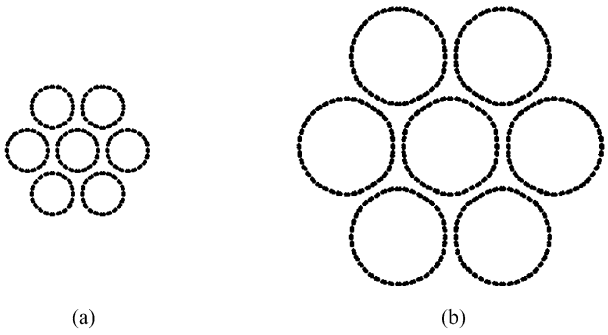

Fig. 6. Cross-section of (a) a (10,10) SWCNT bundle and (b) a (20,20) SWCNT bundle system after each has been relaxed.

Fig. 7. Snapshots of the twist of the SWCNT bundle.

the cross-section, and therefore more atoms are in close contact. This is due to the tensile loading component in the axial direction, similar to that in wire ropes (Fig. 4), which acts as the confinement load that pushes the surrounding tubes to the core. Consequently, this leads to shorter separation and a stronger corrugation effect, as shown in the molecular mechanics study.

5.2. Enhancement in load transfer

Due to the complication associated with the deformed geometry, it will be difficult to obtain an estimation using the MM approach presented in Section 2. However, the effect of the twist on the load transfer can be directly measured from the simulation. Here we use the "transferred load" as an index for the efficiency of the load transfer. The transferred load is defined as the axial load that is passed on to the core tube for a particular twisted SWCNT bundle structure. If there is little load transfer between the core and surrounding tubes, it is expected that the magnitude is going to be small since the contact is essentially smooth. On the other hand, if the load is such that the core tube can be loaded up to its tensile strength, then the load transfer mechanism is very efficient. Following this concept, further simulations were performed on a bundle of SWCNTs with the same cross-sectional configuration as in the last section but with a length of 153.72 Å. The total number of atoms is 17,500. Both ends of the core tube are fixed and a twist around the center of the core on the six neigh-

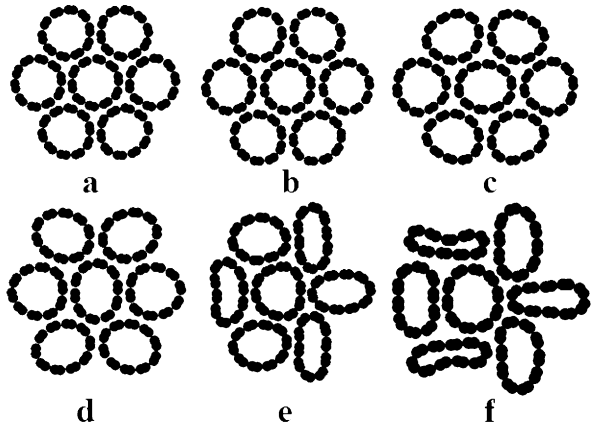

Fig. 8. Change in cross-section at the mid-length of the SWCNT bundle as a function of twist angle.

boring SWCNTs is applied to achieve a given angle of twist. After this, the whole twisted structure is relaxed with the two ends fixed. After the rope is completely relaxed, a constant incremental displacement is then imposed on the core tube while holding the six surrounding nanotubes fixed. The whole process is solved as a quasi-static problem using an implicit algorithm. In the quasi-static algorithm, the equilibrium structure is obtained for each incremental step by ignoring the inertia effect and the corresponding transferred load is then evaluated. This load is obtained by summing up all the axial components of the force acting on the core tube due to the non-bonded interaction. The relaxed structure is obtained using the conjugate gradient method.

To quantify the magnitude of the twist, we define the twist angle as the relative twist between the two ends of the bundle. A total of eight cases have been studied, which correspond to total twisting angles of 0, 30, 60, 90, 120, 150, 180 and 210°. Plotted in Fig. 9 are the axial load transferred to the inner tube as a function of the twist angle. As can be seen in Fig. 9, small twist has very little effect. For the case of 0 degrees (no twist) a force of only ~0.048 eV/Å is transferred to the center tube, an indication of a very smooth inter-tube contact condition; however, for a twist angle of 120° the transferred load increases to 1.63 eV/Å, about 34 times higher. Our calculation also indicates that too much twist results in unstable structures, i.e., the inner tube is being squeezed out when the twisting angle is 180° or higher. For the least-squares linear fitting we plotted in Fig. 9 along with the original data points, it is indicated that the transferred load increases 13.5 meV/Å for one degree of twist before 120°, and decreases 25.4 meV/Å for each additional degree of twist after that until 210° of twist. This calculation clearly indicates that a great enhancement in the load transfer mechanism can be achieved by having a nano-rope with a certain threshold value of helical angle of twist. Recently, Pipes and Hubert [31] have applied both textile mechanics and anisotropic elasticity to analyze continuous CNTs assembled in helical geometry. The effective elastic properties were predicted and their study showed the strong dependence of the mechanical behavior on the helical angle of the assembly.

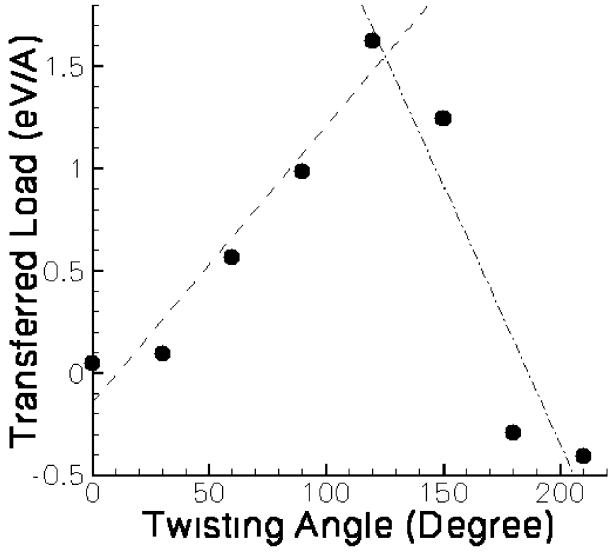

Fig. 9. Transferred load as a function of twisting angle (the dashed and dash-botted lines are the linear fitting for the strengthening and weakening stage of the load transfer).

6. Conclusions

The load transfer mechanism in SWCNT bundles was studied using both molecular mechanics, and molecular dynamics. The major focus was the effect of inter-tube interaction on the transfer of load. The simulation revealed that the radial deformation strongly depends on the twist angle, which consequently changes the nature of the contact and contributes to a new interlayer tribology. An interesting possibility for collapsed nanotubes is that the effective (that is, "engineering") stiffness and possibly strength, will increase simply because there is less empty space—inside the tubes and between them. We advocate experiments whose aim is growing larger diameter SWCNTs that may naturally collapse into ribbons, and rests on their tribology when in the form of ropes.

We summarized two factors that contribute to this inter-tube interaction, namely surface tension and shear strength. The contact length necessary to ensure an effective load transfer has a close relation to the corrugation effect, which depends on the inter-tube gap. A shorter gap leads to stronger corrugation and therefore better load transfer. Based on the simulations presented in this paper, we predict that significantly higher load bearing capacity in tension can be achieved by making ropes and textiles of SWCNTs.

Acknowledgements

RSR and WKL acknowledge the support from the grant: Nanorope Mechanics, NSF No. 0200797 (Oscar Dillon and Ken Chong, Program Managers). RSR appreciates support from the NASA Langley Research Center "Computational Materials: Nanotechnology Modeling and Simulation Program," by the "NASA University Research, Engineering and Technology Institute on Bio Inspired Materials (BIMat) under award No. NCC-1-02037." The work of DQ has also been supported by the grant from NSF, the Tull Family Endowment, Dissertation Year Fellowship from Northwestern University, and the Ohio Board of Regents.

References

[1] Iijima S. Helical microtubules of graphitic carbon. Nature 1991; 354(6348):56–8.

[2] Hone J, Whitney M, Zettl A. Thermal conductivity of single-walled carbon nanotubes. Synthetic Metals 1999;103(1–3):2498–9.

[3] Berber S, Kwon YK, Tomanek D. Unusually high thermal conductivity of carbon nanotubes. Physical Review Letters 2000; 84(20):4613–6.

[4] Qian D, Wagner GJ, Liu WK, Yu MF, Ruoff RS. Mechanics of carbon nanotubes. Applied Mechanics Review 2002;55(6):495–533.

[5] Qian D, Dickey EC, Andrews R, Rantell T. Load transfer and deformation mechanisms in carbon nanotube-polystyrene composites. Applied Physics Letters 2000;76(20):2868–70.

[6] Ajayan PM, Schadler LS, Giannaris C, Rubio A. Single-walled carbon nanotube–polymer composites: strength and weakness. Advanced Materials 2000;12(10):750–53.

[7] Yu MF, Yakobson BI, Ruoff RS. Controlled sliding and pullout of nested shells in individual multiwalled carbon nanotubes. Journal of Physical Chemistry B 2000;104(37):8764–7.

[8] Cumings J, Zettl A. Low-friction nanoscale linear bearing realized from multiwall carbon nanotubes. Science 2000;289(5479):602–4.

[9] Kelly BT. Physics of graphite. London: Applied Science; 1981.

[10] Dal HJ, Rinzler AG, Nikolaev P, Thess A, Colbert DT, Smalley RE. Single-wall nanotubes produced by metal-catalyzed disproportionation of carbon monoxide. Chemical Physics Letters 1996;260(3–4):471–5.

[11] Thess A, Lee R, Nikolaev P, Dai H, Petit P, Robert J, et al. Crystalline ropes of metallic carbon nanotubes. Science 1996; 273(5274):483–7.

[12] Yakobson BI. Personal communication. 2001.

[13] Ausman KD. Personal communication. 2001.

[14] Piner RD. Personal communication. 2001.

[15] Geohegan DB, Schittenhelm H, Fan X, Pennycook SJ, Puretzky AA, Guillorn MA, et al. Condensed phase growth of single-wall carbon nanotubes from laser annealed nanoparticulates. Applied Physics Letters 2001;78(21):3307–9.

[16] Qin LC, Iijima S. Twisting of single-walled carbon nanotube bundles. Materials Research Society Symposium Proceedings 2000;593:33–8.

[17] Costello GA. Theory of wire rope. 2nd ed. New York: Springer; 1997.

[18] Salvetat JP, Briggs GAD, Bonard JM, Basca RR, Kulik AJ, Stockli T, et al. Elastic and shear moduli of single-walled carbon nanotube ropes. Physical Review Letters 1999;82(5):944–7.

[19] Girifalco LA, Lad RA. Energy of cohesion, compressibility and the potential energy functions of the graphite system. Journal of Chemical Physics 1956;25(4):693–7.

[20] Girifalco LA. Molecular-properties of C-60 in the gas and solid-phases. Journal of Physical Chemistry 1992;96(2):858–61.

[21] Yu MF, Lourie O, Dyer MJ, Moloni K, Kelly TF, Ruoff RS. Strength and breaking mechanism of multiwalled carbon nanotubes under tensile load. Science 2000;287(5453):637–40.

[22] Tersoff J, Ruoff RS. Structural-properties of a carbon-nanotube crystal. Physical Review Letters 1994;73(5):676–9.

[23] Wang Y, Tomanek D, Bertsch GF. Stiffness of a solid composed of C60 clusters. Physical Review B 1991;44(12):6562–5.

[24] Qian, D, Liu, WK, Ruoff, RS. Mechanics of C60 in nanotubes. Journal of Physical Chemistry B, 2001, 105, 10753-10758.

[25] Tang J, Qin LC, Sasaki T, Yudasaka M, Matsushita A, Iijima S. Compressibility and polygonization of single-walled carbon nanotubes under hydrostatic pressure. Physical Review Letters 2000;85(9):1887–9.

[26] Maniwa Y, Fujiwara R, Kira H, Tou H, Kataura H, Suzuki S, et al. Thermal expansion of single-walled carbon nanotube (SWNT) bundles: X-ray diffraction studies—art.no. 241402. Physical Review B 2001;6424(24):p. art. no.-241402.

[27] Isaac D. Personal communication. 2002.

[28] Institute A.I.A.S. Wire rope users manual. 1979, Washington, DC.

[29] Yu MF, Kowalewski T, Ruoff RS. Investigation of the radial deformability of individual carbon nanotubes under controlled indentation force. Physical Review Letters 2000; 85(7):1456–9.

[30] Brenner, DW. Empirical potential for hydrocarbons for use in simulating the chemical vapor-deposition of diamond films. Physical Review B, 1990, 42(15), 9458-9471.

[31] Pipes BR, Hubert P. Helical carbon nanotube arrays: mechanical properties. Composites Science and Technology 2002;62(3):419–28.

[32] Lopez MJ, Rubio A, Alonso JA, Qin LC. Novel polygonized single-wall Carbon Nanotube bundles. Physical Review Letters 2001;86(14):3056–9.

[33] Shenderov O, Brenner DW, Ruoff RS. Would diamond nanorods be stronger than fullerene nanotubes? Nanoletters [in press].